Geochemistry of soils formed on ophiolite rocks in the Al-Bassit region of Northwestern Syria

Dr. Samar Ghanem [*]
Dr. Ahlam Ibrahim [**]

□ ABSTRACT □

The al-Bassit region is characterized by ophiolite rocks with distinct chemical compositions and characteristics. Six soil profiles formed on ophiolite rocks (basic and ultra-basic) were selected to determine the chemical composition and intensity of weathering processes in these soils. Nineteen samples of profiled soil were selected, and some of their morphological, physical, and chemical properties were studied. Weathering indexes were also calculated (CIA, WIP, CIW…), The results showed that the behavior of chemical elements is influenced by parent materials, and that all profiles are generally located within the weak weathering range, especially profiles P4 and P1, which are derived from basalt and serpentine rocks, respectively. Except for profile P3, which is derived from fine-grained gabbro rocks, it has been exposed to moderate-intensity weathering.

Keywords: Parent materials - Weathering - Soil geochemistry - Mineral composition - Weathering index.

[*] **Assistant Professor, Department of Soil and Land Reclamation, Faculty of Agricultural Engineering, Tishreen University, lattakia-Syria. samar.ghanem@tishreen.edu.sy**
[**] **Associate Professor, Department of Geology, Faculty of Science, Tishreen University, lattakia -Syria. ahlam.ibrahim@tishreen.edu.sy**

جيوكيمياء الترب المتشكلة على صخور الأفيوليت
في منطقة البسيط – شمال غرب سوريا

د. سمر غانم *

د. أحلام إبراهيم **

◻ ملخّص ◻

تتميز منطقة البسيط بوجود صخور الأفيوليت التي لها تركيب وخصائص كيميائية مميزة. تم اختيار ستة مقاطع للترب المتشكلة على صخور الأفيوليت (الأساسية وفوق الأساسية) بهدف معرفة التركيب الكيميائي وكثافة عمليات التجوية في هذه الترب. تم اختيار تسعة عشر عينة من الترب المدروسة، ودراسة بعض خواصها المورفولوجية والفيزيائية والكيميائية، كما تم حساب بعض مؤشرات التجوية (CIA، WIP، CIW...)، أظهرت النتائج أن سلوك العناصر الكيميائية يتأثر بالمواد الأم، وأن جميع المقاطع تقع بشكل عام ضمن نطاق التجوية الضعيفة، خاصة المقاطع P4 وP1، المشتقة من صخور البازلت والسربنتين، على التوالي. باستثناء المقطع P3، المشتق من صخور الغابرو ناعم الحبات، فقد أظهر تعرضاً للتجوية معتدلة الشدة.

الكلمات المفتاحية: المواد الأم – التجوية – جيوكيمياء التربة – التركيب المعدني – مؤشر التجوية.

---

*مدرسة – قسم التربة واستصلاح الأراضي، كلية الهندسة الزراعية، جامعة تشرين، سورية samar.ghanem@tishreen.edu.sy .

**أستاذ مساعد– قسم الجيولوجيا – كلية العلوم– جامعة تشرين– سورية ahlam.ibrahim@tishreen.edu.sy .

Introduction

Soil formation is a dynamic process rather than a static process, in which soil develops through dynamic interaction between air, water, parent material and organisms. If one or more of these major factors changes, the soil will be different (Tunçay *et al.,* 2019). In particular, changes in parent materials can affect many soil properties under local conditions because of their mineralogical and textural variation (Birkeland, 1999; Dengiz & Usul, 2018).

Soil is generally considered a by-product of the physical, chemical, and biological weathering of rocks and metals on or near the Earth's surface. (Pope *et al.,* 2002; Yatsu, 1988; Tunçay & Dengiz, 2016)

Weathering rates depend on the rock composition, temperature range, and amount of precipitation.

To quantitatively determine the degree of development of the soil profile, it is necessary to estimate the state of the initial parent material (Al-Makki, 2016)

In order to estimate the degree of development of the soil profile by measuring the physical, chemical and mineralogical changes that take place during the transformation of the parent material into soil. Several methods are available for determining the homogeneity of the parent material, one of which is the measurement of the chemical weathering indicators of the parent material and the depth distribution of oxides (Barshad, 1964).

Chemical weathering indices, which use quantitative measurements based on total rock chemical analyses, are commonly used to characterize the intensity and mechanism of weathering (Nesbitt and Young, 1982; Irfan, 1996; 1999; Ng *et al.,* 2001; Gupta & Rao, 2001; Voicu & Bardoux, 2002), compare the extent of the chemical change between different materials (Birkeland, 1999; Munroe *et al.*, 2007; Darmody *et al.,* 2005; Schatz *et al.*, 2015), and evaluate soil fertility and development (Delvaux *et al.*, 1989).

Chemical weathering indices estimate the intensity of soil chemical weathering by comparing changes in major and trace element concentrations as ratios of mobile (Na_2O, K_2O, MgO, CaO) to relatively immobile elements (TiO_2, SiO_2, Al_2O_3, Fe_2O_3) in soil and parent material (Duzgoren-Aydin *et al*., 2002; Price & Velbel, 2003; Yang *et al.,* 2004). Typically, studies that use indices of alteration focus on the change of the index with depth in a weathering profile (Price & Velbel, 2003).

Most weathering indicators decrease with an increase in the degree of weathering, considering that some indicators, such as the Weathering Index (Harnois, 1988), show an increasing trend according to the type of inputs in the weathering index.

This study aims to estimate the degree of weathering of the parent material and the development of soil profiles formed over the ophiolitic rocks in the Al-Bassit region, by calculating weathering indicators and the behavior of some elements .

Materials and Methods

1 Location and characterization of the study area

Soils were sampled in the Al-bassit area in the northwestern part of Syria (Figure 1), between the coordinates: N: 35° 41`, E: 35° 42`- N: 35° 57`, E: 36° 05`.The climate of the studied area is described as a Mediterranean climate. The mean annual rainfall of approximately 750–1250 mm is concentrated between December and February, whereas June and August are the driest months (Fares *et al.,* 1991).
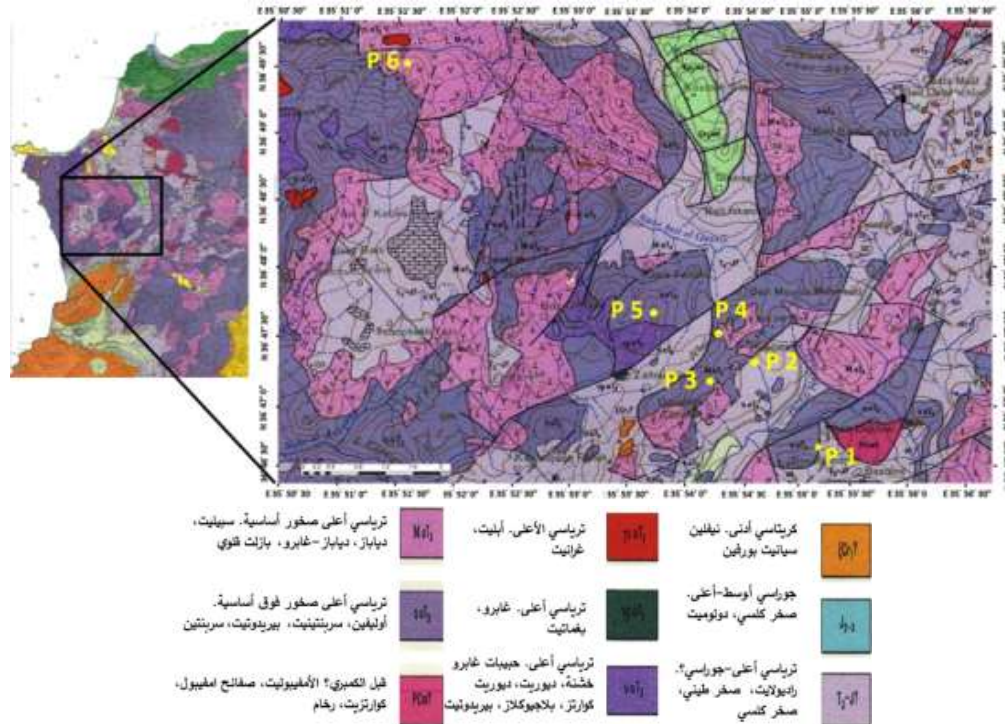
**Figure 1. Location of the studied area in Al-Bassit map 1/50000
(Ponikarov et al. ,1962), and soil profile distribution.**

The soil moisture regime is Xeric, whereas mesic is the temperature soil regime
(Ilaiwi, 1983). The vegetation cover is mainly pine forest. Soil profiles were dug on
various parent materials selected on the basis of the geological map of Al-Bassit at a scale
of 1/50000. The soil profile P1 is derived from ultramafic rock (serpentinized peridotite),
whereas the other profiles are all derived from mafic rocks (P2, P3, P5 and P6 are derived
from gabbro rocks and P4 is derived from basalt rocks) Table 1.

Table 1. Description of the sites of the studied profiles.

Profile	Parent material	Land cover
P1	Serpentinized peridotite	Pine forest
P2	Fine-grained pegmatite gabbro	Pine forest
P3	Coarse-grained pegmatite Gabbro	Pine forest
P4	Basalt	Pine forest
P5	Coarse-grained pegmatite gabbro	Pine forest
P6	Pegmatite gabbro	Pine forest

2. Soil profile description and soil sampling
The Global Positioning System (GPS) was used to record altitude and geographic
locations. The soil morphology of each horizon of the profiles was described according to
(Schoeneberger et al., 2012). Soil samples were collected, air-dried, ground, sieved
through a 2-mm mesh to obtain air-dried fine soil, and physically and chemically analyzed.
3 Physical and chemical analyses
Chemical and physical analyses of soil samples include: percentage of water content and
particle distribution using the hydrometer method (FAO, 1974). Soil reaction pH (H_2O)
was determined using a pH –meter of a 1:2.5 suspension, total carbonates were measured

by using volumetric titration (Drouineau, 1942). Organic matter was determined according to the (FAO, 1974) method.

4 Calculation of chemical weathering indices

Nineteen fresh representative samples were selected for chemical analysis. The percentages of SiO_2, Al_2O_3, Fe_2O_3, CaO, MgO, K_2O, and Na_2O in soil and parent material were determined by X-ray fluorescence at the General Company for Cement Manufacture and Building Materials (GCCMBM), Tartous, Syria, according to Karathanasis and Hajek (1996).

Numerous chemical weathering indices were used to quantify the chemical weathering intensity. These indices were calculated on the basis of the molecular proportions of major element oxides. Each oxide's molecular proportion can be easily calculated from the percentage of oxide based on molecular weight (Shao *et al*., 2012). Table 2 lists the weathering indices evaluated in this study.

Table 2: The weathering index evaluated in current study.

Index	Formula	Reference
R	SiO_2/Al_2O_3	(Ruxton, 1968)
Si/Sesq.	$SiO_2/Al_2O_3+Fe_2O_3$	(Birkeland ,1999)
CIA	$[Al_2O_3/(Al_2O_3 + Na_2O + CaO^*+K_2O)] \times 100$	(Nesbitt and Young, 1982)
CIW	$[Al_2O_3/(Al_2O_3 + Na_2O + CaO^*)] \times 100$	(Harnois, 1988)
WIP	$[(2Na_2O/0.35) (MgO/0.9) (2K_2O/0.25) (CaO^*/0.7)] \times 100$	(Parker, 1970)

R = (Fe2O3+ Al2O3), Seisq = (Fe2O3+ Al2O3).
CaO* represents the CaO contained only in the silicate fraction.

Results and Discussion

1 Morphological properties:

Different morphological features were present in the research region, (horizons thickness, color, and surface horizon depth), Table 3. The morphological descriptions of studied profiles are:

Horizons thickness: The results showed that the thickness of surface horizons varied based on the physiographic position of the pedon and pedogenic and geomorphological processes, notably topography, had a significant impact on soil structure ranging from granular in the surface horizons to subangular blocky in subsurface horizons.

Soil color: is closely reflective of the parent material. The color intensity (Value) in profiles was equal to (2, 3, 4). These low values are due to the ferromagnesian minerals of the parent material, in addition to the presence of organic matter in the surface horizons, and the oxidation processes in some profiles. Chroma values are also low and are between (1-4).

Soil structure: The granular structure was distinguished in all surface horizons of all profiles, whereas it was blocky in subsurface horizons.

Soil horizons and their boundaries were identified and described in the field, at the time of taking the profiles images (table 3). Horizontal boundaries are described in terms of **distinctness** (which refers to the thickness of the zone within which the boundary is located) and **topography** (which refers to the irregularities of the boundary between horizons).

Distinctness can be defined in 5 classes: very abrupt (< 0.5 cm), abrupt (0.5 to 2 cm), clear (2 to 5 cm), gradual (5 to 15 cm), and diffuse (> 15 cm) (Schoeneberger *et al*., 2012).

Table3 Some morphological properties of studied profiles.

Profile	Depth (cm)	Color		Structure	Boundary	Special features
		(dry)	(moisture)	(grade, size, type)	Topography/ distinctness	
P1	0-15	10YR 4/2	10YR3/2	2 Mgr	s/d	Transported fragments on the surface
	15-55	5Y6/4	5Y 4/3	3 Msbk	s/c	Residual of parent material developed structure
	55-95	5YR 5/8	2.5Y4/2	3M sbk	-	
P2	0-20	5Y 4/2	5Y 3/2	2Fgr	w/d	
	20-55	5Y 5/3	5Y 4/3	3 M sbk	w/g	Iron oxides
	55-90	5Y 5/3	5Y 4/3	3 Msbk	-	Iron oxides
P3	0-5	7.5YR 4/3	7.5YR 3/3	3F gr	s/g	Iron oxides
	5-40	7.5YR 3/4	5YR 4/4	3Msbk	s/c	Iron oxides
	40-75	2.5Y 6/4	2.5Y 4/4	3 Msbk	-	
P4	0-5	10YR3/3	10YR3/4	3F gr	i/c	
	5-20	5YR4/4	5YR3/4	3Fsbk	s/g	Rocky structure
	20-95	5YR4/4	5YR3/4	3Msbk	-	Rocky structure
P5	0-10	10YR3/2	10YR2/1	2F gr	s/g	
	10-30	5Y 4/2	5Y 3/2	2M gr	w/c	
	30-60	5Y 4/4	5Y 3/2	3 Msbk	s/g	
	60-85	صخري			-	
P6	0-15	7.5YR 3/2	7.5YR 2/2	1F gr	s/g	
	15-55	7.5YR 4/2	7.5YR 3/2	3Msbk	s/d	Some mottles
	55-95	10YR 7/6	10YR 4/3	3 Msbk	-	Some mottles

Abbreviations: Boundary: a = abrupt; c = clear; g = gradual; d = diffuse; s = smooth; w = wavy; i = irregular. Structure: Grade- 3: strong, 2: moderate, 1: weak. Size- F: fine, M: medium. Type-, sbk: subangular blocky, gr: granula.

Four types of topography are being used: smooth (a plane with few or no irregularities), wavy (has undulations in which depressions are wider than they are deep), irregular (has pockets that are deeper than they are wide), and broken (discontinuous or interrupted boundaries) (Schoeneberger *et al.*, 2012). In the studied profiles topography was smooth generally, wavy in profiles P2, P5, and irregular in profile P4. Distinctness was generally gradual, and clear between horizons of profiles P3, P6.

2. Physical and chemical properties

The results of the laboratory analysis of the physical and chemical properties in table 4 show that the pH values were neutral. The water content varied between horizons and was associated with the organic matter and clay amount. The percentage of organic carbon in profiles took a natural direction and decreased with depth.

The total carbonate percentage decreased in the studied profiles. This percentage increased slightly in P1 formed from serpentine rocks. This is due to the alteration of this ultramafic rock (Zedef *et al.*, 2000)

The percentage of sand was high in the horizons of the studied profiles, except P3, and this is due to the composition of the mineral parent material and the immaturity of profiles. In the P3 profile (pegmatitic gabbro parent material) the percentage of clay increased, due to the transformations of the minerals constituting the parent material

(Schwertmann & Taylor, 1989; Coleman & Jove, 1992), which reflects greater development of this profile than other profiles.

The total carbonate percentage decreased in the studied profiles. This percentage increased slightly in P1 formed from serpentine rocks. This is due to the alteration of this ultramafic rock (Zedef *et al.*, 2000)

The percentage of sand was high in the horizons of the studied profiles, except P3, and this is due to the composition of the mineral parent material and the immaturity of profiles. In the P3 profile (pegmatic gabbro parent material) the percentage of clay increased because of the transformations of the minerals constituting the parent material (Schwertmann & Taylor, 1989; Coleman & Jove, 1992), which reflects greater development of this profile than other profiles.

Table 4. Some soil physical and chemical properties of studied profiles.

Profile	Depth (cm)				%				Soil texture
P1		pH	Water content	OM	Total carbonate	Clay	Silt	Sand	
	0-15	7.67	5.76	1.07	3.75	46	25	29	**Clay**
	15-55	7.69	10.88	1.34	20	37	22	41	**Clay loam**
	55-95	7.5	4.48	0.67	30	10	23	67	**Sandy loam**
P2	0-20	7.92	17.89	1.2	20	20	21	59	**Sandy clay loam**
	20-55	7.35	3.92	0.83	7.5	12	10	78	**Sandy loam**
	55-90	7.61	5.03	0.6	5	14	17	69	**Sandy loam**
P3	0-5	7.64	3.9	1.21	11.25	47	16	37	**Clay**
	5-40	7.5	3.4	0.34	2.5	71	15	14	**Clay**
	40-75	7.79	4.3	0.28	3.75	24	23	53	**Sandy clay loam**
P4	0-5	7.57	4.13	1.97	7.5	8	12	80	**Loamy sand**
	5-20	7.81	4.42	0.87	12.5	6	14	80	**Loamy sand**
	20-95	7.66	4.16	0.47	3.75	8	16	76	**Sandy loam**
P5	0-10	7.44	5.03	4	10	39	28	33	**Clay loam**
	10-30	7.44	5.03	0.7	8.75	24	29	47	**Loam**
	30-60	7.51	3.43	1.34	17.5	16	27	57	**Sandy loam**
	60-85	7.74	4.32	0.67	17.5	6	10	84	**Loamy sand**
P6	0-15	7.3	3.6	5	3.75	28	19	53	**Sandy clay loam**
	15-55	7.98	4.2	1.67	2.5	33	12	55	**Clay loam**
	55-95	7.03	3.12	1.34	2.5	16	11	73	**Sandy loam**

3. Chemical composition

The percentage of silica was almost constant in the horizons of the studied profiles and within the natural limits of the soils formed on this type of rock. Generally, the percentage of silica is related to the parent material and topography (Sidhu *et al.*, 2000). Its percentage ranged between (35.51 - 45.22%) (table 5). The highest percentage of silica (45.22%) is found in the P5 profile formed from pegmatitic gabbro parent material (figure 2). There was a loss of silica in the surface horizons of the P4 profile.

Table 5 Chemical composition as a percentage of the sampled soils and parent materials.

| | | \%| | | | | | | | | | |
		SiO_2	Al_2O_3	Fe_2O_3	CaO	MgO	K_2O	Na_2O	SO_3	Cl	H_2O	LOI	Sum
P1	0−15	40.29	3.77	13.6	6.98	10.03	0.24	0.76	0.14	0.04	9.2	22.94	81.85
	15−55	41.89	3.84	14.29	6.22	15.67	0.14	0.75	0.13	0.04	11.6	21.95	82.98
	55−95	41.53	10.31	9.59	6.45	12.5	0.44	0.74	0.13	0.03	13.2	18.68	81.71
Average		41.24	5.97	12.49	6.55	12.73	0.27	0.75	0.13	0.04	11.33	21.19	82.18
P2	0−20	41.02	8.82	9.73	10.95	10.86	0.13	0.92	0.15	0.07	5.9	20.44	82.67
	20−55	40.95	9.21	8.89	10.93	11.67	0.02	1.02	0.14	0.04	6.7	21.31	82.89
	55−90	41.02	9.71	8.6	10.19	12.11	0.01	1.07	0.12	0.04	20.6	21.2	82.88
Average		41.00	9.25	9.07	10.69	11.55	0.05	1.00	0.14	0.05	11.07	20.98	82.81
P3	0−5	39.51	13.58	12.45	8.64	5.47	0.26	1	0.15	0.03	5.4	12.75	81.1
	5−40	39.29	16.82	14.01	7.46	4.41	0.17	0.88	0.14	0.04	4.9	10.66	83.23
	40−75	44.32	6.51	11.23	10.09	10.51	0	0.78	0.13	0.03	8.4	19.38	83.58
Average		41.04	12.30	12.56	8.73	6.80	0.14	0.89	0.14	0.03	6.23	14.26	82.64
P4	0−5	35.51	11.57	18.01	7.36	6.29	0.16	0.89	0.14	0.036	6.3	12.63	79.96
	5−20	39.71	11.23	17.61	7.38	4.77	0.11	0.91	0.14	0.03	8.5	10.99	81.88
	20−95	37.28	11.64	19.57	6.86	5.23	0.02	0.74	0.12	0.03	7.8	11.09	81.5
Average		37.50	11.48	18.40	7.20	5.43	0.10	0.85	0.13	0.03	7.53	11.57	81.11
P5	0−10	44.39	9.45	11.1	8.89	7.2	1.1	1.3	0.18	0.05	7.5	14.78	83.57
	10−30	43.6	9.07	10.6	9.6	7.2	0.8	1.2	0.20	0.04	10.8	15.29	82.23
	30−60	45.45	8.95	10.6	9	8.7	0.6	1.2	0.13	0.03	9.9	16.56	84.72
	60−85	44.32	9.48	11.1	9.1	8	0.2	1	0.12	0.03	10.7	15.87	83.92
Average		44.44	9.24	10.85	9.15	7.78	0.68	1.18	0.16	0.038	9.73	15.63	83.61
P6	0−15	43.87	8.13	9.47	11.11	9.1	0.15	0.9	0.14	0.03	4.8	18.64	82.92
	15−55	45.22	7.04	9.16	11.35	10.82	0.06	0.81	0.14	0.04	3.4	20.71	84.65
	55−95	39.14	14.19	12.62	10.39	5.62	0.03	1.1	0.18	0.04	6	14.28	83.3
Average		42.74	9.79	10.42	10.95	8.51	0.08	0.94	0.15	0.04	4.73	17.88	83.62

The percentage of iron and aluminum oxides is second, after silica, and the highest percentages were in profile P4 formed from basaltic parent material.

There was an accumulation of iron oxide in the soil horizons of P1 profile, and a loss of aluminum oxide in the P6 profile, compared with the parent material. In the P3 profile (pegmatitic gabbro parent material), an accumulation of aluminum and iron oxides was observed, in the center of the profile, which was morphologically reflected on the coloration of the soil of the profile in red, with a loss of calcium and magnesium oxides, which can be attributed to the biogeocycling of the elements and the activity of weathering processes (Asio & Jahn, 2007).

There was an accumulation of magnesium oxide in the soil horizons of the P1 and P6 profiles, compared with the parent material. In contrast, in the P3 profile, the highest percentage was found in the parent material.

In general, the percentages of calcium oxides were relatively low, especially in P1 formed on serpentine (figure 2), which is due to the nature of the mineral composition of the parent material. The percentage of calcium oxide was close between the horizons of the same

profile, except for profile P3, in which this percentage in the horizons of the soil was less than that of the parent material (figure 3), which may be due to its exposure to a leaching process.

The percentage of sodium and potassium oxides decreased in the soil profiles, which is due to the rapid movement and leaching of these two elements, especially in the prevailing climatic conditions in the region.

The molecular ratios of SiO_2/R_2O_3 were almost constant between horizons of one profile except for profiles P3 and P6.

A decrease in the values of $SiO_2/R_2O_3$was observed within the surface horizons of profile P3, which indicates the activity of weathering processes and accumulation of $Fe_2O_3+Al_2O_3$. In contrast, this percentage increased in the surface horizons of profile P6, which reflects the occurrence of liberation and leaching of these oxides with the activity of the weathering process.

The molecular ratio $[CaO+MgO+K_2O/SiO_2+Fe_2O_3+Al_2O_3]$ was almost constant between horizons of one profile, and ranged between (0.15-0.37). This percentage increased in the surface horizons of profile P4 (Not exposed to much weathering) compared to the parent material.

The results in Table 6 show that a high molecular ratio MgO/CaO were in all horizons of studied profiles, as a result of the richness of the parent materials in ferromagnesian minerals. The highest values of this ratio were in P1 formed on serpentine, especially in the center of the profile, with the following values (3.22–3.53 -2.71), and according to the sequence of horizons.
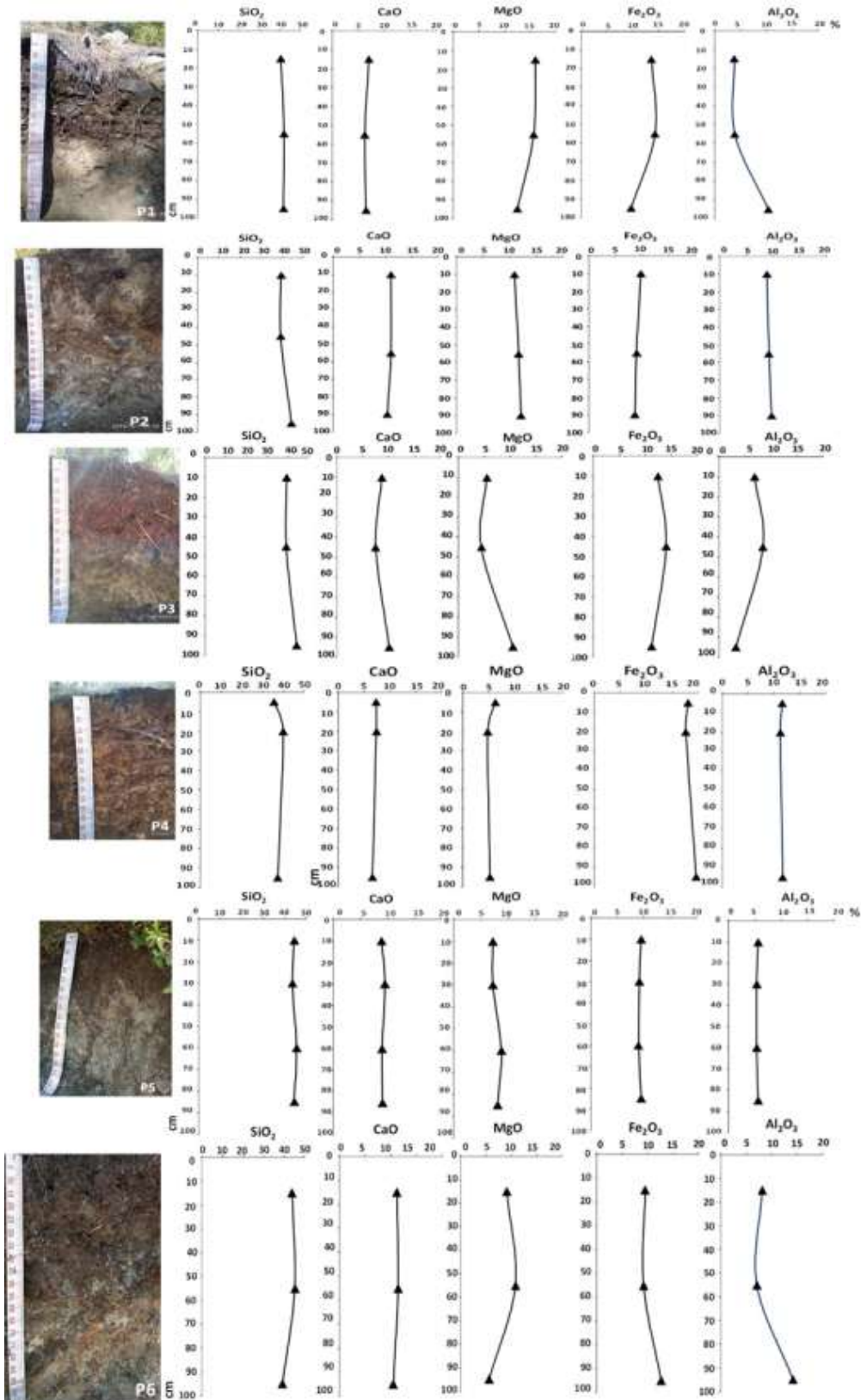
Figure 2. Percentage change of some major element oxides in soil profile horizons with depth.

**Table 6 Some chemical weathering indices in the horizons of the studied profiles**

Profile	Depth (cm)	R	SiO₂/R	SiO₂/Al₂O₃	SiO₂/Fe₂O₃	CIA	CIW	WIP	MgO/CaO	CaO+MgO+K₂O/ SiO₂+ Fe₂O₃+Al₂O₃
P1	0-15	0.12	5.51	18.17	7.90	20.95	21.26	71.38	3.22	0.18
	15-55	0.13	5.50	18.55	7.82	23.20	23.41	67.50	3.53	0.15
	55-95	0.16	4.30	6.85	11.55	43.40	44.30	61.74	2.71	0.15
P2	0-20	0.15	4.64	7.91	11.24	28.99	29.13	67.69	1.39	0.25
	20-55	0.15	4.68	7.56	12.28	29.89	29.91	69.87	1.49	0.26
	55-90	0.15	4.59	7.18	12.72	32.43	32.44	69.03	1.66	0.24
P3	0-5	0.21	3.12	4.95	8.46	43.46	43.86	48.66	0.89	0.20
	5-40	0.25	2.59	3.97	7.48	52.50	52.80	40.84	0.83	0.16
	40-75	0.13	5.51	11.57	10.52	24.91	24.91	61.94	1.46	0.22
P4	0-5	0.23	2.62	5.22	5.26	27.06	43.76	172.45	1.20	0.37
	5-20	0.22	3.01	6.01	6.01	30.04	42.91	128.46	0.90	0.29
	20-95	0.24	2.63	5.44	5.08	43.07	46.58	54.34	1.10	0.18
P5	0-10	0.17	4.40	6.79	12.53	36.37	37.78	63.37	1.13	0.21
	10-30	0.16	4.53	7.00	12.82	34.30	35.27	62.29	1.05	0.22
	30-60	0.16	4.74	7.29	13.54	35.70	36.51	63.77	1.35	0.20
	60-85	0.17	4.38	6.76	12.47	37.63	37.94	56.70	1.23	0.20
P6	0-15	0.14	5.26	9.17	12.35	27.09	27.24	63.19	1.15	0.25
	15-55	0.13	5.97	10.92	13.16	24.18	24.24	66.99	1.33	0.25
	55-95	0.22	2.99	4.69	8.27	40.59	40.63	52.51	0.76	0.23

The value of the indicators CIA and CIW increased in the surface horizons of the third profile compared to the parent material, indicating the activity of the weathering process in these horizons (figure3). The lowest values of these indicators were in the horizons of the fourth profile.

The indicator (WIP) took an opposite direction (figure3), and its values were lowest in the horizons of the third profile and highest in the horizons of the fourth profile.

Generally, rocks from the upper crust and unweathered igneous rocks have CIA values of ~ 50, whereas the soils and sediments derived from intensely weathered rocks, and containing residual clay minerals such as kaolinite and/or gibbsite, have CIA values approaching 100 (Fedo *et al*., 1995; Kalinin *et al*., 2021; Özaytekin *et al*., 2012). Soils with CIA values of (50 to 60) are classified as very slightly weathered, slightly weathered (60 to 70), moderately weathered (70 to 80), highly weathered (80 to 90), and extremely weathered (90 to100) (Nesbitt & Young, 1982).

In the profiles examined in the current study, the CIA values varied from 20.95 in the P1 profile to 52.5 in the P3 profile.
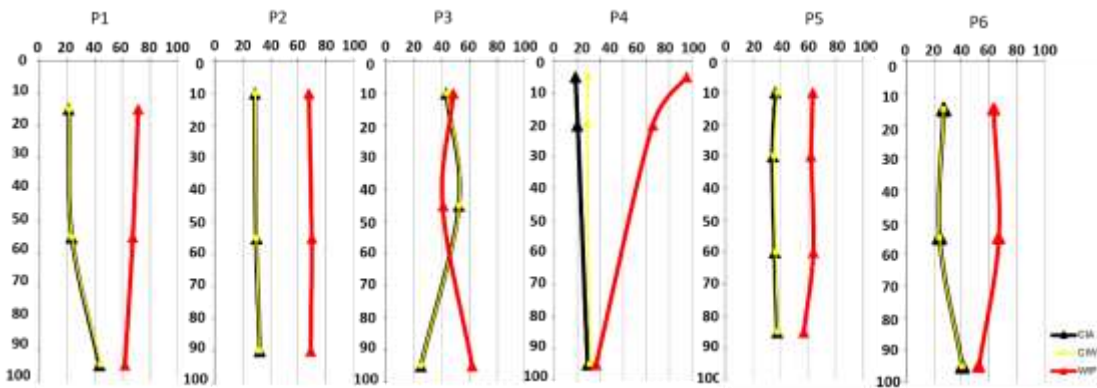
Figure 3 Changes of weathering indices CIA, CIW and WIP values with depth for soil samples derived from ophiolitic rocks.

When the interrelationship between (WIP) and (CIA) was (figure 4) it was found that the surface horizons of all profiles, except for profile P3, were very slightly weathered.
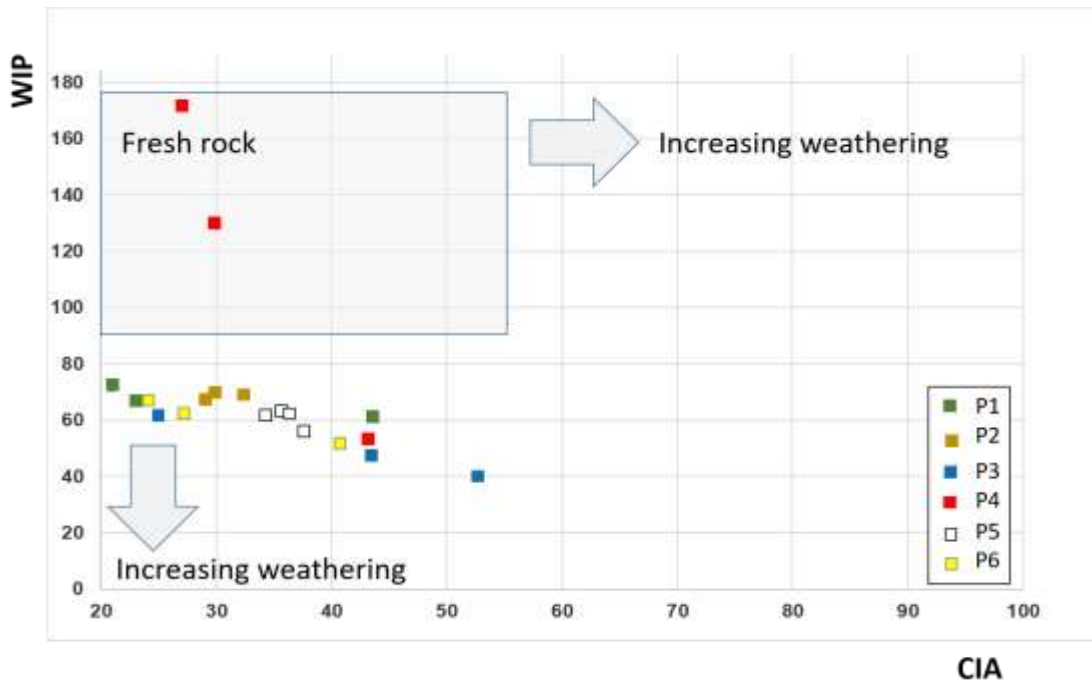
Figure 4 Interrelationship between two weathering proxies- weathering index of Parker (WIP) and chemical index of alteration (CIA) for soil samples derived from ophiolitic rocks (Babu *et al.,* 2021).

The research samples were applied to a triangular diagram A-CN-K, based on (Nesbitt & Young., 1984; Fedo *et al.,*1995; Lambe, 1996; Peng, 2023; Borges *et al.*, 2008). It was found that profiles samples are all positioned on line A- CN, which reflects the high initial abundance of CaO and Na$_2$O in these samples.

Samples of the surface horizons of profile P3 (gabbro-pegmatite) are located close to the smectite composition, reflecting high concentrations of alumina-bearing minerals and intermediate weathering of calcium and sodium minerals of this profile in a Mediterranean climate. The ophiolite trend does not intersect the A-K joint, which reflects very low initial values of K in the parent material. All other profiles samples fall into the weak weathering range (Figure 5)
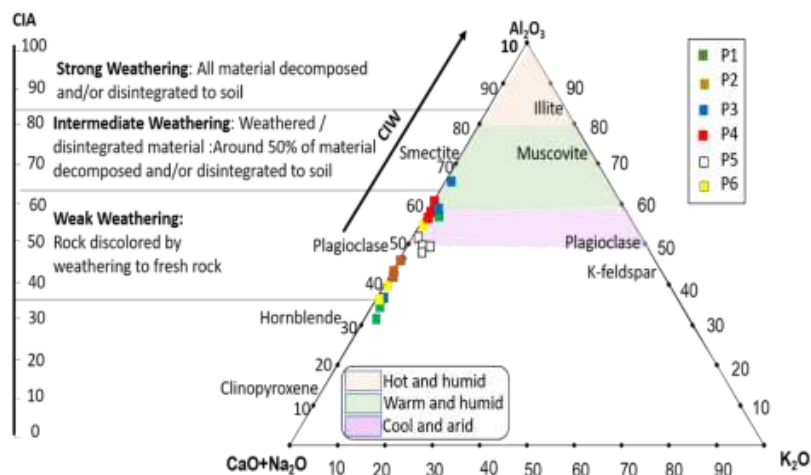

Figure 5 A-CN-K ternary diagram of molecular proportions of Al2O3- (CaO + Na2O)-K2O for studied soils (Nesbitt & Young., 1984; Fedo et al.,1995; Lambe., 1996; Peng, 2023; Borges et al., 2008) shown at the side is the CIA scale (Nessbit & Young, 1982). The CIA scale is divided into the simplified typical weathering profile described by the Geological Society of London in Lambe (1996).

Nesbitt and Young (1989) introduced an A–CNK–FM diagram to illustrate the relationship between leucocratic and melanocratic constituents in weathering (figure 6).
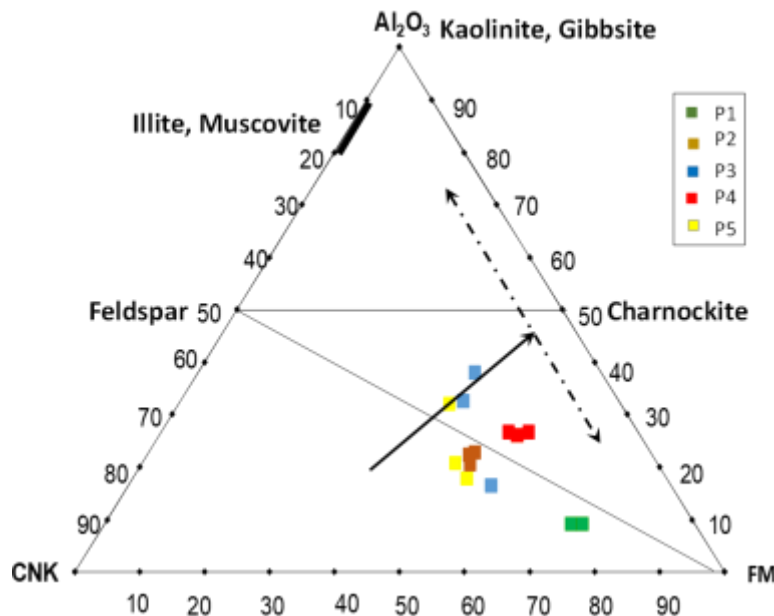

Figure (6) A–CNK–FM diagram showing the weathering of ophiolitic soils in Al- Bassit region (Nesbitt and Young, 1989; Nesbitt et al., 1996). A-A2O3; CNK - CaO* + Na2O + K2O; FM — FeO* (total FeO) + MgO.

The line Feldspar–FM represents the joining of feldspar to FM [FeO* (total FeO) + MgO]. Solid arrows show general trends with increasing weathering. Dashed arrows represent subsequent depletion or enrichment from the general weathering trend. The vertices correspond to the molecular ratios.

The A–CNK–FM diagrams showed that profiles samples tends to the vertex FM of the triangle, which reflects the high content of ferromagnesian minerals of parent materials, particularly in profile P1 (derived from serpentinized peridotite). P3 profile (Coarse-grained pegmatite gabbro) has the highest percentage of alumina, which reflects the richness of this profile in aluminosilicate minerals resulting from the development of weathering processes, (Fig. 6; Table 5).

Conclusion:

In general, according to the morphological characteristics studied, the profiles were in the early stages of development.

In the P3 profile (pegmatic gabbro parent material), the percentage of clay increased because of the transformations of the minerals constituting the parent material, which reflects greater development of this profile than other profiles.

the chemical composition showed that the percentage of iron and aluminum oxides is second after silica.

The behavior of chemical elements is influenced by the parent materials. There was an accumulation of iron and magnesium oxides in the soil horizons of the P1 profile (serpentine). In the P3 profile (gabbro), an accumulation of aluminum and iron oxides was observed,

The interrelationship between (WIP) and (CIA) and the indicator (WIP) revealed that the surface horizons of all profiles, except for profile P3, were very slightly weathered.

The triangular diagram A-CN-K shows that samples of the surface horizons of profile P3 (gabbro-pegmatite) had high concentrations of alumina-bearing minerals and intermediate weathering of calcium and sodium minerals. All other profiles samples fall into the weak weathering range.

The A–CNK–FM diagrams showed the high content of ferromagnesian minerals of parent materials, particularly in profile P1 (derived from serpentinized peridotite).

References:

AL-MAKKI M R. Parent material and weathering of rendzina soils in Al Jabel Al Akhdar region, Libya. 2016, Vol. 12, No 3, p. 881-889.

ARISTIZÁBAL E, ROSER B & YOKOTA S. Tropical chemical weathering of hillslope deposits and bedrock source in the Aburrá Valley, northern Colombian Andes. *Engineering Geology*. 2005, *81*(4), 389-406.

ASIO V B & JAHN R. Weathering of basaltic rock and clay mineral formation in Leyte, Philippines. Philipp Agric Sci. 2007, 90 (3), 222-230.

BABU L, MOHAN S V, MOHAN M & PRADEEPKUMAR A P. Highly mature sediments in the tropical monsoonal environment of southwestern India: an appraisal based on weathering indices. Ecofeminism and Climate Change. 2021, 2 (2), 69-82.

BARSHAD I. Chemistry of soil development. 1964. P. 1-70. In F.E. Bear (ed.) Chemistry of the soil. Reinhold, New York.

BIRKELAND PW. Soils and Geomorphology, Third edition. New York, Oxford University Press. 1999, 430 P.

BORGES J B, HUH Y, MOON S, NOH H. Provenance and weathering control on river bed sediments of the eastern Tibetan Plateau and the Russian Far East. – Chemical Geology. 2008, 254, 52-72.

BUGGLE B, GLASER B, HAMBACH U, GERASIMENKO N, MARKOVIC S. An evaluation of geochemical weathering indices in loess-paleosol studies. Quaternary International. 2011, 240: 12-21.

CHESWORTH W. The parent rock effect in the genesis of soil. Geoderma. 1973, 210, 215.

COLEMAN R G, AND JOVE C. Geological origin of serpentinites. In: Baker AJM, Proctor J, Reeves RD (eds) The vegetation of ultramafic (Serpentine) soils: Proceedings of the First International conference on serpentine ecology. Intercept, Andover, Hampshire. 1992.

DARMODY RG, THORN CE AND ALLEN CE. Chemical weathering and boulder mantles, Kärkevagge, Swedish Lapland. Geomorphology. 2005, 67, 159–170.

DELVAUX B, HERBILLON AJ, VIELVOYE L. Characterization of a weathering sequence of soils derived from volcanic ash in Cameroon. Taxonomic, mineralogical and agronomic implications. Geoderma. 1989, 45, 375 – 388.

DENGIZ O, USUL M. Multi-criteria approach with linear combination technique and analytical hierarchy process in land evaluation studies. Eurasian Journal of Soil Science. 2018, 7(1). 20-29.

DROUINEAU G. Dosage rapide du calcaire actif du sol. Nouvelles données sur la reportation de la nature des fraction calcaires. Ann. Agron. 1942, 12: 411–450.

DUZGOREN-AYDIN NS, AYDIN A, MALPAS J. Re-assessment of chemical weathering indices: case study on pyroclastic rocks of Hong Kong. *Engineering Geology.* 2002, 63 (1-2), 99-119.

FARES F, ABEIDO M, HABIB H, BATHA A. Study of the lands and forests of the coastal region using remote sensing techniques, Latakia Governorate (inventory, evaluation, and uses). 1991, 183 P.

FAO. The Euphrates Pilot Irrigation Project. *Methods of soil analysis, Gadeb Soil Laboratory (A laboratory manual).* Food and Agriculture Organization, Rome, Italy. 1974.

FEDO CM, NESBITT HW & YOUNG GM. Unraveling the effects of potassium metasomatism in sedimentary rocks and paleosols with implications for paleoweathering conditions and provenance. Geolog. 1995, 23, 921–924.

GUPTA A, RAO K. Weathering indices and their applicability for crystalline rocks. Bull. Eng. Geol. Environ. 2001, 60, 201 – 221.

HARNOIS, L. The CIW Index: a new chemical index for weathering. Sedimentary Geology. 1988, 55, 319–322.

ILAIWI M. *Contribution to the knowledge of the* soils *of Syria*. Ph. D. thesis, State Univ. of Ghent, Belgium. 1983, 259 P.

IRFAN TY. Mineralogy, fabric properties and classification of weathered granites in Hong Kong. Q. J. Eng. Geol. 1996, 29, 5 – 35.

IRFAN TY. Characterization of weathered volcanic rocks in Hong Kong. Q. J. Eng. Geol. 1999, 32, 317 – 348.

KALININ P I, KUDREVATYKH I Y, MALYSHEV V V, PILGUY L S, BUHONOV A V, MITENKO G V & ALEKSEEV A O. Chemical weathering in semi-arid soils of the Russian plain. 2021, CATENA, 206, 105554.

KARATHANASIS A D AND HAJEK B F. Elemental analysis by X-ray fluorescence spectroscopy. Methods of Soil Analysis: Part 3 Chemical Methods. 1996, 5:161-223.

MUNROE S J, FARRUGIA G, RYAN CP. Parent material and chemical weathering in alpine soils on Mt. Mansfield, Vermont, USA. 2007. Catena 70: 39– 48.

LAMBE P. Residual soils. Landslides: investigation and mitigation. In: Turner, K., Schuster, R. (Eds.), Landslides Investigation and Mitigation, Special Report. Transportation Research Board, National Research Council. 1996, vol. 247, pp. 507 – 524.

NESBITT YW, YOUNG G M. Early Proterozoic climates and plate motions inferred from major element chemistry of lutites. 1982*, Nature* 299: 715-717

NESBITT HW, YOUNG GM. Prediction of some 780 weathering trends of plutonic and volcanic rocks based 781 on thermodynamic and kinetic considerations. 782 Geochimica et Cosmochimica Acta. 1984, 48 (7), 1523–1534.

NESBITT H W & YOUNG G M. Formation and diagenesis of weathering profiles. *The Journal of Geology*. 1989, *97* (2), 129-147.

NESBITT HW, YOUNG GM, MCLENNAN SM, KEAYS RR. Effects of chemical weathering and sorting on the petrogenesis of siliciclastic sediments, with implication for provenance studies. J. Geol. 1996, 104, 525 – 542

NG CW, GUAN P, SHANG YJ. Weathering mechanisms and indices of the igneous rocks of Hong Kong. Q. J. Eng. Geol. 2001, 34, 133 – 151.

ÖZAYTEKIN H H & KARAKAPLAN S M. Soil formation on the Karadağ volcano at a semi-arid environment from the Central Anatolia. African Journal of Agricultural Research. 2012, Vol. 7(15), pp: 2283-2296.

PARKER A. An index of weathering for silicate rocks. Geological Magazine. 1970, 107, 501–504.

PENG G, CHEN W, JIA P, LUO M, HE Y, JIN Y, XU C AND SHAN X. Middle-Late Eocene Climate in the Pearl River Mouth Basin: Evidence from a Palynological and Geological Element Record in the Xijiang Main Subsag. Minerals. 2023, 13 (3), 374.

PONIKAROV V; KAZMIN V; KULALAKOV V. Geological map of Syria 1:50000. Technoexport, contact N :944 Moscow. USSR, 1962.

POPE GA, MEIERDING TC & PARADISE TR. Geomorphology's role in the study of weathering of cultural Stone. Geomorphology. 2002, 47,211-225.

PRICE JR, VELBEL M A. Chemical weathering indices applied to weathering profiles developed on heterogeneous felsic metamorphic parent rocks. *Chemical Geology.* 2003, 202 (3-4): 397-416,

PROC. First Int. Conf. Geomechanics in Tropical Lateritic and Saprolitic Soils, Brasilia, vol. 1, pp. 175 – 186.

RUXTON BP. Measures of the degree of chemical weathering of rocks. Journal of Geology. 1968, 76, 518–527.

SCHATZ AK, SCHOLTEN T AND P KÜHN. Paleoclimate and weathering of the Tokaj (NE Hungary) loess paleosol sequence: a comparison of geochemical weathering indices and paleoclimate parameters. Palaeoecology. 2015, Vol. 426: 170–182.

SCHOENEBERGER PJ, WYSOCKI DA, BENHAM EC. Field Book for Describing and Sampling Soils, Version 3.0. USDA Natural Resources Conservation Service, National Soil Survey Center. 2012.

SCHWERTMANN U, AND TAYLOR R M. Iron oxides. In: Dixon, J.B., Weed, S.B., editors. Minerals in soil environments. 2nd. ed. Madison: Soil Science Society of America. 1989, 379-438. (Book Serie, 1).

SHAO J, YANG S, & LI C. Chemical indices (CIA and WIP) as proxies for integrated chemical weathering in China: inferences from analysis of fluvial sediments. Sedimentary Geology. 2012, 265, 110-120.

SIDHU G S, GHOSH S K, & MANJAIAH K M. Pedological variabilities and classification of some dominant soils of Aravallies-Yamuna river transect in semi- arid tract of Haryana. Agropedology. 2000, 10, P:80-87.

SUEOKA T, LEE I K, HURAMATSU M, IMAMURA S. Geomechanical properties and engineering classification for decomposed granite soils in Kaduna district, Nigeria, 1985.

TUNÇAY T & DENGIZ O. Chemical weathering rates and geochemical mineralogical characteristics of soils developed on heterogeneous parent material and toposequence. Carpathian Journal of Earth and Environmental Sciences, 2016, Vol. 11, No 2, p. 583 – 598.

TUNÇAY T, DENGIZ O, BAYRAMIN I, KILIC S, BASKAN O. Chemical weathering indices applied to soils developed on old lake sediments in a semi-arid region of Turkey. Eurasian J. Soil Sci. 2019, 8: 60–72.

VOICU G, BARDOUX M. Geochemical behavior under tropical weathering of the Barama–Mazaruni greenstone belt at Omai gold mine, Guiana shield. Appl. Geochem. 2002, 17, 321 – 336.

XIONG S, DING, Z, ZHU, Y, ZHOU, R, & LU H. A∼ 6 Ma chemical weathering history, the grain size dependence of chemical weathering intensity, and its implications for provenance change of the Chinese loess–red clay deposit. Quaternary Science Reviews. 2010, 29 (15-16), 1911-1922.

YANG SY, Li CX, YANG DY, LI XS. Chemical weathering of the loess deposits in the lower Changjiang Valley China and paleoclimatic implications. Quaternary International, 2004, 117: 27-34.

YATSU E. The nature of weathering an introduction. Tokyo, Sozosha, 1988.

ZEDEF V, RUSSELL M J, FALLICK A E, & HALL A J. Genesis of vein stockwork and sedimentary magnesite and hydromagnesite deposits in the ultramafic terranes of southwestern Turkey: a stable isotope study. Economic Geology. 2000, 95(2), 429-445.